Chemical Engineering Science 306 (2025) 121215

Contents lists available at ScienceDirect

Chemical Engineering Science

journal homepage: www.elsevier.com/locate/ces

Assessing the viability of bio-based adsorbents for PFAS removal

J.B. Roman [a,b], A.J.B. Kemperman [b], W.G.J. van der Meer [b], J.A. Wood [a,*]

[a] Soft Matter, Fluidics and Interfaces, University of Twente, Enschede, Drienerlolaan 5, 7522 NB, Overijssel, the Netherlands
[b] Membrane Technology and Engineering for Water Treatment, University of Twente, Enschede, Drienerlolaan 5, 7522 NB, Overijssel, the Netherlands

ARTICLE INFO

Keywords:
Lignin
Water treatment
Bio-based
Adsorption
PFAS

ABSTRACT

Removal of per- and polyfluoroalkyl substances (PFAS) from water resources is a pressing matter. This work assesses the viability of various bio-based materials for PFAS adsorption and in which scenarios they are preferable over using activated carbon. Lignin was found to be the most promising bio-based adsorbent, having adsorption capacities of 1.6, 4.3, 5.3 ng/g for PFBA, PFBS and PFOA respectively at environmentally relevant concentrations. Following this, carbonization of lignin improved the specific surface area from 5 m^2/g to between 10 and 140 m^2/g. Carbonization improved adsorption capacity by 1 to 2 orders of magnitude depending on the PFAS compound, which can largely be explained by the increased specific surface area. Subsequent column studies showed that the carbonized lignin performed 30 times worse than conventional activated carbon. A simple environmental impact and cost analysis showed that using the carbonized lignin is not preferable over conventional activated carbon.

Glossary

GAC: granular activated carbon
M3PFBA: perfluorobutanoic acid with 3 isotopically labeled carbon atoms
M3PFBS: perfluorobutanesulfonic acid with 3 isotopically labeled carbon atoms
M8PFOA: perfluorooctanoic acid with 8 isotopically labeled carbon atoms
M8PFOS: perfluorooctanesulfonic acid with 8 isotopically labeled carbon atoms
PFAS: per- and polyfluoroalkyl substances
PFBA: perfluorobutanoic acid
PFBS: perfluorobutanesulfonic acid
PFOA: perfluorooctanoic acid
PFOS: perfluorooctanesulfonic acid

1. Introduction

There is increasing concern over the ubiquitous presence of per- and polyfluoroalkyl substances (PFAS) in the water supply of drinking water facilities (Appleman et al., 2014). Furthermore the presence of PFAS is not addressed by many current water treatment facilities (Appleman et al., 2014). Although definitive health impacts in humans have not yet been quantified, animal studies have shown harmful effects of several PFAS (ATSDR, 2021; Schrenk et al., 2020). By disposal of PFAS compounds into surface waters, these compounds can end up in both crops and plants, since some PFAS are strongly bio-accumulative (Felizeter et al., 2012; Li et al., 2022). Therefore the widespread distribution of PFAS in both drinking water and food leads to exposures of whole populations to these compounds (Calafat et al., 2007).

PFAS as a group of compounds are defined by the C-F bonds in their structure. Due to the large electronegativity of the fluorine atom C-F bonds are extremely strong, making PFAS compounds highly chemically stable as well as possessing omniphobic behavior. These characteristics have led to their widespread use in both industry and consumer products (Kotthoff et al., 2015; Whitehead et al., 2021). The properties of the C-F backbone also lead to different interactions, compared to conventional hydrocarbons, between PFAS and non-fluorinated compounds as well as between different PFAS themselves (Nakayama and Hasegawa, 2023). Hydrophobic interactions alone cannot explain the complex adsorption behavior observed for the case of PFAS compounds (Nakayama and Hasegawa, 2023). Furthermore, many PFAS are amphiphilic in nature, with the most studied molecules having a mostly linear fluorocarbon chain and a sulfonic or carboxylic end group. This hydrophillic end group provides large solubility and mobility in water, while still retaining high chemical stability and resistance to biodegradation (Wackett, 2021).

Currently the only widely employed method for removal of PFAS from water is adsorption onto activated carbons (Franke et al., 2021;

* Corresponding author.
E-mail address: j.a.wood@utwente.nl (J.A. Wood).

https://doi.org/10.1016/j.ces.2025.121215
Received 10 October 2024; Received in revised form 7 January 2025; Accepted 11 January 2025

Available online 14 January 2025

Vakili et al., 2021). However, the use of activated carbons can be challenging from a economical perspective (Franke et al., 2021) and unsustainable from an environmental perspective (Kim et al., 2019). Most activated carbons are current derived from fossil sources (peat, coal, etc.) (EU consortium PortableCrac, 2018). A rapid breakthrough of smaller PFAS (fewer than 6 carbon atoms, such as perfluorobutanoic acid) (McCleaf et al., 2017) and degradation of the adsorption capacity of granular activated carbon (GAC) over its lifetime (Yuan et al., 2022), lead to difficulties for complete removal of the spectrum of PFAS compounds typically encountered. Consequently current drinking water treatment plants using activated carbons have shown mixed success regarding PFAS removal (Boone et al., 2019; Chen et al., 2022). One of the causes for this is the general negatively charged nature of activated carbon adsorbents and the most prevalent PFAS compounds being anionic in nature, leading to electrostatic repulsion (Aumeier et al., 2023).

Previously Fabregat et al. described adsorption of PFAS at low concentrations to various carbonaceous adsorbents (Fabregat-Palau et al., 2022). They concluded that PFAS adsorption to carbonaceous adsorbents is mostly governed by hydrophobic interactions, since the chain length of the PFAS anion was strongly correlated with the equilibrium coefficient (Fabregat-Palau et al., 2022), while electrostatic interaction played a minor role. In contrast with Fabregat et al., Zhang et al. found that electrostatic interactions played a major role for the adsorption of PFAS compounds, while also finding that hydrophobic interactions are of influence to the performance (Zhang et al., 2022). It could be that the positively charged carbonaceous adsorbent of Zhang et al. changed the behavior from being dominated by hydrophobic effects to electrostatic interactions.

Other methods for PFAS remediation being investigated are aimed at more selective removal. For example, anion exchange resins can be used which are able to bind the negatively charged group of acidic PFAS (Wang et al., 2019). These materials are more able to retain short-chain PFAS than non-selective materials like activated carbons (Gagliano et al., 2020). Just like carbonaceous adsorbents, these adsorbents are also subject to an equilibrium (Donnan equilibrium) between adsorbed species and species in solution, where other ions also compete for the same adsorption sites. Therefore ion containing streams will be difficult to treat using ion-exchange resins, as there are orders of magnitude difference in the concentrations of PFAS and salt ions generally. Another group of selective materials that has been explored is fluorinated compounds, the rationale being that by incorporating fluorinated groups, the adsorbent will have higher affinity for PFAS than for competing organic pollutants (Kumarasamy et al., 2020). Whether producing more PFAS compounds in order to address PFAS pollution is a viable and sustainable approach is at present unknown (Verduzco and Wong, 2020). Another common approach for PFAS removal is concentrating the PFAS using membranes (nanofiltration or reverse osmosis) or foam fractionation (McCleaf et al., 2023; Buckley et al., 2023; Franke et al., 2021). However, these technologies do not actually remove PFAS from water, but rather displace them to a more concentrated stream (the retentate of the membrane or the foam layer in the case of foam fractionation), where removal or destruction is more feasible by for example adsorption.

Previously Li et al. (2021) showed that both environmental and monetary benefits can be achieved by using bio-based adsorbent materials (Li et al., 2021). The most used bio-based material is activated carbon produced from coconut shells. One of the major benefits of using cheap bio-based adsorbents is that regeneration of the adsorbents becomes less critical for economic viability. Consequently, this allows for more aggressive treatment options to destroy the adsorbed PFAS compounds, while worrying less about the reuse of the adsorbent material. Furthermore the use of fossil based adsorbent materials is not a practice that is ultimately sustainable (Mantripragada et al., 2022). Therefore there is a strong need to find renewable materials that can function as adsorbent or as feedstock for production of carbonaceous adsorbents, that can lead to environmental and possibly also economical benefits.

A substantial amount of research has already been devoted to the testing and tailoring of bio-based adsorbents (mostly biochars), in order to produce a product comparable to conventional activated carbon (Fabregat-Palau et al., 2022; Bergna et al., 2022; Thauront et al., 2024). In this research we investigated the ability of several unmodified bio-based materials to adsorb PFAS at environmentally relevant concentrations and compare this to a conventional adsorbent. The hypothesis is that even though the bio-based materials likely have a lower adsorption capacity, the environmental benefits of using bio-based materials could outweigh the need for additional adsorbent material. Plant fibres and their derivatives like cellulose and lignin are attractive adsorbents due to their wide availability, coming from the production of cellulose in the paper industry, where the by-product lignin is often burned. Lignin has been previously used for heavy metal adsorption in wastewater treatment (Wang et al., 2021), showing its possible application as an adsorbent. Although lignin is generally a heterogeneous product (Wang et al., 2021), the main backbone of the lignin involves phenolic groups. The adsorption capacity of these materials is investigated at PFAS levels which are found in water resources and benchmarked to adsorption on activated carbon. Batch testing was performed to screen a wide array of materials and investigate the isotherms of a few promising adsorbents. Following this we carbonized the lignin material to enhance its surface area and compare it with the base material. The carbonized lignin and an activated carbon were then used in rapid small scale column testing to assess the adsorbents in a more applied setting. Finally we analyze the global warming potential of adsorption on the bio-based lignin material and the carbonized version of it we produced and compare it to the conventional use of activated carbon.

2. Materials and methods

PFAS chemicals (PFOA (≥ 98%), PFBA (98%), PFBS (98%) and PFOS (≥ 98%), see glossary for description of acronyms) were acquired from Sigma-Aldrich and isotopically labeled internal standards (M8PFOA, M3PFBA, M3PFBS and M8PFOS) were aquired from Greyhound Chromatography (produced by Wellington Laboratories, Guelph, Canada). The PFOS was found to be a mixture of a linear and branched products, of which only a single branched product was found in significant quantities (26%) (Schulz et al., 2020). Methanol and acetonitrile were of LC-MS grade (>99.9%, Optima brand) and formic acid was ACS grade (96%), all obtained from Fisher Scientific. Ammonium hydroxide (28-30% in water) and potassium chloride (99.5%) were obtained from Sigma-Aldrich and HPLC grade ammonium acetate was obtained from Merck (Lichropur). The adsorbents used are pulverised activated carbon (CASP-F, Norit), lignin produced from Miscanthus Giganteus by Miscancell BV, the Netherlands and a carbonized version of this lignin material. Chitosan (Sigma Aldrich, medium molecular weight, 75-85% deacetylated), graphene nanoplatelets (Nanografi) and iron-oxide nanoparticles (Nanografi, 14-29 nm) were also investigated, results can be found in the supplementary information. Cellulose fibres (Arbocel B-600, JRS group) were used as adsorbent and as a packing material for flow through tests, similar to the use of glasswool.

Before surface area characterization adsorbents were dried in a vacuum oven at 60 °C (for lignin samples) or in an oven at 200 °C for at least 2 hours before measuring. The samples were then degassed under gentle N_2 flow at 150 °C for at least 8 hours. Surface area characterization measurements were performed using N_2-BET on a Micrometrics Gemini VII. Microporous samples (carbonized lignins and activated carbons) were analyzed by Delft Solid Solutions B.V. using a Micromeritics Tristar II 3020. The density of carbonized lignin and activated carbon were determined using helium pycnometry using a Micrometrics AccuPycII 1340.

The lignin adsorbent was analyzed by thermogravimetric analysis on a NETZSCH STA 449F3. The temperature was increased from room temperature to 1000 °C at a rate of 20 °C/minute. A flow of 70 mL/min of N_2 was used during the initial part of the analysis. After 90 minutes

the N_2 atmosphere was switched to an air atmosphere by flowing 56 mL/min of N_2 and 14 mL/min of O_2. In the air environment, part of the non-volatile carbon can be burned off as CO_2, to give an indication of the fixed carbon amount in the material. What remains is the inorganic material in the sample together with the carbon that did not form gaseous products, such as graphitic carbon.

2.1. Batch adsorption experiments

Adsorption experiments were performed in glass vials on a vortex mixer (VWR advanced mini shaker 15). Adsorbents were added to the vials, after which a PFAS solution was spiked into the vial and the total liquid volume was increased to 15 mL using Milli-Q water (with or without added KCl). The pH of the solutions was not adjusted and was measured before adding the adsorbent material as 5.3 ± 0.4. Initial PFAS concentrations for the isotherm studies were 50, 125, 200, 300, 500 and 1000 ng/L. When evaluating the effect of ionic strength on PFAS adsorption on carbonized lignin the initial concentrations were 50, 100, 200, 400, 600, 800, 1000, 1200, 1400 and 1600 ng/L. It must be mentioned that for the determination of the isotherms for carbonized lignin, the initial concentration of PFOA was 10 times higher than intended. The samples were vortex mixed for at least 100 hours at 220 rpm, as initial screening showed all adsorbents reached equilibrium within 2 days. Afterwards they were left to sediment for 10 minutes after which 10 mL was taken from the supernatant for analysis of the PFAS concentrations.

2.2. PFAS analysis

Due to large matrix effects and convoluted peaks observed when using the native lignin compound as an adsorbent, a cleanup procedure of the samples was required to selectively analyze the PFAS compounds (Kaiser et al., 2020). This was not necessary when the lignin was carbonized or activated carbon was used, where using internal standards for each compound sufficed. For the experiments with native lignin, prior to analysis, solid phase extraction (SPE) was performed using 'Oasis PFAS WAX' cartridges (6cc, 150 mg, 30 µm particle size, obtained from Waters). Samples were mixed with an equal volume of 0.2 M formic acid, sonicated for 20 minutes and then centrifuged for 10 minutes at 6000 rpm (4185 x g, Corning LSE compact centrifuge) before loading onto the cartridges. Cartridges were first equilibrated using 6 mL 0.1 vol% NH_4OH in MeOH, followed by 6 mL of MeOH and 6 mL of 0.1 M formic acid. After drying the cartridge by flowing through air, the samples (20 mL) were loaded by applying a light vacuum at 1-3 drops/s. Following this the cartridges were washed with 6 mL of 0.1 M formic acid, 6 mL of 0.1 M formic acid/MeOH (60/40) and 6 mL of 0.01 vol% NH_4OH in Milli-Q. The cartridges were then dried by pulling through air after which neutral compounds were eluted with 6 mL of pure methanol. This methanol fraction was discarded after which the cartridges were dried again. Thereafter the target compounds were eluted using 3x 6 mL of 0.1 vol% NH_4OH in acetonitrile. The acetonitrile was then evaporated under a gentle nitrogen flow at 60 °C and the samples were reconstituted in 1 mL of 10% methanol and 5 mM ammonium acetate in Milli-Q (HPLC eluent A). It was ensured that the 1 mL of liquid contacted all the glass surface where PFAS might have been deposited during evaporation.

Analysis of PFAS concentrations after adsorption was done by HPLC-MS/MS. HPLC (Ultimate 3000, Thermo Fisher) was performed on a Acclaim RSLC 120 C18 column (Thermo Fisher, 100 x 2.1 mm, 2.2 µm particle size), coupled to a triple quadrupole MS (TSQ Quantis, Thermo Fisher). The flow rate was set at 0.5 mL/min and the column temperature was kept constant at 40 °C with a post column cooler at 30 °C. The injection volume was 50 µL and the needle was washed by a mixture of 25% acetonitrile, 25% methanol, 25% isopropanol and 25% Milli-Q. The eluents were 10% methanol in Milli-Q water with 5 mM ammonium acetate (eluent A) and pure methanol (eluent B). The mobile phase started at 100% A and the gradient was as follows (min,%A): 0, 100%; 1.25, 100%; 1.875, 92%; 5.5, 20%; 7, 20%; 8.45, 100%; 11, 100%.

2.3. Rapid small scale column testing

For rapid small scale column testing, the adsorbents were loaded into empty solid phase extraction (SPE) tubes (6 mL, Merck) fitted with polypropylene frits (VWR). On top of the adsorbent layer, an additional layer of cellulose fibres was added to prevent re-suspension of the adsorption bed when filling the tubes with liquid. Experiments with SPE tubes with only cellulose fibres showed negligible adsorption of PFAS compounds (results in supplementary information). A Harvard syringe pump with 50 mL syringes was used as a feed pump for the filled SPE tubes. In order to ensure complete wetting of the adsorption bed, 4 mL of solution was first added to the tube before connecting the pump. This ensured the solution was always in complete contact with the top of the adsorption bed, although the feed entered the tube irregularly via drops. The feed concentration used in the experiments was 800 ng/L of each of the 4 different PFAS compounds. The output from the column was collected in a glass vessel through a polypropylene needle. At certain intervals, depending on the flowrate, the output was collected through a stainless steel needle with a 2 or 10 mL syringe attached. Experiments were performed using a flowrate of 0.3 mL/min, which corresponds to approximately 30 seconds of contact time. This contact time is similar to the contact time in different experiments we are conducting, results of which will be published later. Although a contact time of 30 seconds is much shorter than what would typically be employed in an industrial setting, it does allow for screening the applicability of different adsorbents multiple times in a practical time scale (Benstoem et al., 2017).

2.4. Data analysis

Batch experiments were analyzed by fitting an isotherm equation to the adsorbed amount-concentration datasets. The adsorbed amount (m_{PFAS}) per amount of adsorbent added ($m_{adsorbent}$) was calculated from the measured equilibrium concentration by:

$$\frac{m_{PFAS}}{m_{adsorbent}} = (C_0 - C_{eq})V \tag{1}$$

Here m_{PFAS} is the adsorbed mass of a PFAS compound (ng), $m_{adsorbent}$ is the adsorbent mass used in (g), C_0 is the PFAS concentration in the liquid at t = 0 (ng/L), C_{eq} is the measured liquid equilibrium concentration (ng/L) and V is the solution volume (L). Afterwards the adsorbed amount of PFAS is normalized by the adsorbent mass used. Using these values, isotherms were fit between the normalized amount of mass adsorbed and the equilibrium concentration. In this work, we made use of the Langmuir isotherm (equation (2)) and a linear isotherm (which the Langmuir isotherm reduces to at very low concentrations, equation (3)). The Langmuir isotherm assumes the adsorbent contains a set amount of homogeneous adsorption sites on which exactly one molecule can adsorb per site (Langmuir, 1918). The maximum adsorption capacity is reached when all sites are occupied, forming a non-interacting layer of adsorbed molecules (Langmuir, 1918). A strong fit to the Langmuir isotherm indicates that the adsorbate has stronger interactions with the adsorbent than with itself (Hubbe, 2021). The Langmuir isotherm tends to work well at low concentrations of pollutants adsorbing on similar sites, but breaks down when molecules have strong intermolecular interactions leading to multilayer adsorption. Since the linear isotherm is a limiting case of the Langmuir isotherm, the same underlying assumptions apply.

$$\frac{m_{PFAS}}{m_{adsorbent}} = \frac{K_D N_{max} C_{eq}}{N_{max} + K_D C_{eq}} \tag{2}$$

$$\frac{m_{PFAS}}{m_{adsorbent}} = K_D C_{eq} \tag{3}$$

Here K_D is the distribution coefficient (L/g), N_{max} is the maximum adsorption capacity (ng/g) and C_{eq} is the equilibrium concentration (ng/L). It is important to note that since the equilibrium concentration is used for calculating the amount of adsorbed PFAS (equation (1)), both are subject to measurement error and these errors are highly correlated (Bolster, 2008). To account for errors in both variables, fitting the non-linear Langmuir model to the collected data was done in Origin (version 2021b) using the 'orthogonal distance regression' option. The linear isotherm model was fit using both standard linear regression and orthogonal distance regression with negligible difference, due to the effect of accounting for errors in C_{eq} being non-consequential (likely due to the high correlation between errors in x and y).

For analysis of the flow through adsorption experiments the Thomas model was used (Thomas, 1948). The Thomas model is based on the assumption of plug flow through the column and uses pseudo-second-order (in case of a Langmuir isotherm) or first-order (in case of a linear isotherm) kinetic representation of adsorption (Thomas, 1948). These kinetic representations simultaneously account for internal mass transfer, external mass transfer and adsorption kinetics. It therefore does not allow to differentiate between these effects (Hiester and Vermeulen, 1952). The equations derived by Thomas were put into a more practical form by Hiester and Vermeulen (1952) (Hiester and Vermeulen, 1952). The equations in the case of a linear isotherm are:

$$\frac{C}{C_0} = J(s,t) \tag{4}$$

$$J(x,y) = 1 - \int_0^x \exp(-y-\xi) I_0(2\sqrt{y\xi}) d\xi \tag{5}$$

$$s = \frac{\kappa \epsilon V_{bed}}{\phi_V} \tag{6}$$

$$t = \frac{\kappa \epsilon V}{K_D \rho_s \phi_V} \tag{7}$$

Here C is the measured concentration (ng/L), C_0 is the measured feed concentration (ng/L), I_0 is the zero-order Bessel function of the first kind, κ is a kinetic rate constant (1/s), ϵ is the bed void fraction, V_{bed}, ϕ_V is the flowrate (L/s), V is the treated volume (L), K_D is the distribution coefficient (L/g) and ρ_s is the solid particle density (g/L). The parameter D_g, which represents the ratio of concentrations on solid and in fluid phase at saturation, used by Hiester and Vermeulen was exchanged for the distribution coefficient K_D via:

$$D_g = \frac{K_D \rho_s}{\epsilon} \tag{8}$$

Since PFAS compounds are present at low concentrations (ng/L) a linear isotherm will often hold, however some situations can ask for a maximum adsorption capacity to be included. In these situations the Thomas model based on the Langmuir isotherm is used:

$$\frac{C}{C_0} = \frac{J(rs,t)}{J(rs,t) + \exp(r-1)(t-s)[1-J(s,rt)]} \tag{9}$$

$$\text{with: } r = \frac{1}{1+K_D C_0} \tag{10}$$

$$t = \frac{\kappa \epsilon V (1+K_D C_0)}{N_{max} K_D \rho_s \phi_V} \tag{11}$$

$$\text{with: } D_g = \frac{N_{max} K_D \rho_s}{(1+K_D C_0)\epsilon} \tag{12}$$

3. Results and discussion

3.1. Comparison of adsorbent materials

Our goal was to compare different bio-based and conventional adsorbents to assess the viability of bio-based materials for PFAS removal, even if they are not specifically fabricated for usage as an adsorbent. An overview of adsorption capacities of all the adsorbents tested can be found in the supplementary information, where comparisons were made by extrapolation or interpolation (depending on the mass of adsorbent used) of the data at different adsorbent amounts towards a value of 1 g of adsorbent used. Both chitosan and lignin were the only bio-based materials with a significant adsorption capacity, the cellulose materials did not show any significant adsorption of PFAS. Lignin had a higher adsorption capacity than chitosan for all compounds except PFBA, for which adsorption capacity was similar. The similarity of adsorption capacity of PFBA even though the specific surface area of chitosan was 25 times smaller than that of lignin, indicates that the cationic nature of chitosan governed its adsorption performance through electrostatic interactions (Shahrokhi and Park, 2024). On the other hand the lower adsorption capacity of PFBA for lignin indicates that predominantly hydrophobic interactions determine the PFAS adsorption to lignin. Due to its overall higher adsorption capacity, we concluded that lignin was the most promising candidate to test further, from the selection of bio-based adsorbents used. The remainder of this work will therefore focus on the usage of lignin as an adsorbent.

Table 1
Adsorbents used with corresponding specific surface area and particle size.

Adsorbent	SSA (m^2/g)	particle size
Miscanthus Lignin	5.1	1 mm
Carbonized Lignin	10.7 / 140[1]	10 μm / 1 mm
Activated Carbon	1592[1]	20 μm
Cellulose fibres	0.6	20 x 200 μm
Chitosan	0.2	200 μm
Graphene nanoplatelets	733	4 μm
Ironoxide nanoparticles	66.2	5 μm

[1] these adsorbents are microporous and therefore the determination of the N_2-BET surface area is complicated. For carbonized lignin there was also a lot of batch to batch variation, the surface areas of the 2 batches used for adsorption experiments are shown. A discussion of N_2-BET surface area determination for these materials is provided in the supplementary information.

3.1.1. Adsorbent preparation and characterization

For each of the adsorbents the specific surface area was determined using the N_2-BET method, the results of which can be seen in Table 1. The large differences in specific surface area between different materials allow for determination of the contribution of purely surface area to PFAS adsorption. We found a lot of batch to batch variation in the specific surface area (10 s to 100 s of (m^2/g)) of the carbonized lignin (more information in the supplementary information). The value of the specific surface area of carbonized lignin given here is of the sample used when making the isotherms.

Thermogravimetric analysis of the lignin was done in order to assess its fixed carbon content and inorganic content, see Fig. 1. The amount of volatile matter was about 50%, the amount of fixed carbon 25% and the leftover ash after burning the carbon content was 20% of the original mass. Whether the inorganic compounds in the ash were increased in mass due to oxidation is unknown.

Following the thermogravimetric analysis some of the material was carbonized in both a pure nitrogen environment, in air or a combination of both. From Fig. 1 the temperature of 600 °C was selected, as at that point most volatile matter has left the material. For this purpose, initial treatment in a tube furnace was done in either a nitrogen or air environment at 600 °C for 3 hours with a ramp rate of 20 °C/min. Part of the material which was carbonized in a nitrogen environment was afterwards treated in air at 400 °C for 30 minutes, again with a ramp rate of 20 °C/min, following the finding by Wang et al. (2023) that short air oxidation of biochar created from softwood led to large increases in adsorption effectiveness (Wang et al., 2023). The remaining mass of these treatments for 5 different locations inside of the tube furnace (numbers increase in the length of the tube, in gas flow direction, a schematic

Table 2
Results of miscanthus lignin carbonization in air, nitrogen or combined environment.

Oven location	Mass remaining (nitrogen) 600 °C, 3 hrs	Mass remaining (nitrogen) 600 °C, 4 hrs	Mass remaining (air) 400 °C, 30 min	Mass remaining (nitrogen → air) 4 hrs + 30 min
1	43.0%	37.5%	31.2%	11.7%
2	43.9%	37.8%	40.7%	15.4%
3	45.0%	38.0%	41.3%	15.7%
4	44.4%	38.3%	53.5%	20.5%
5	44.3%	38.9%	65.9%	25.7%

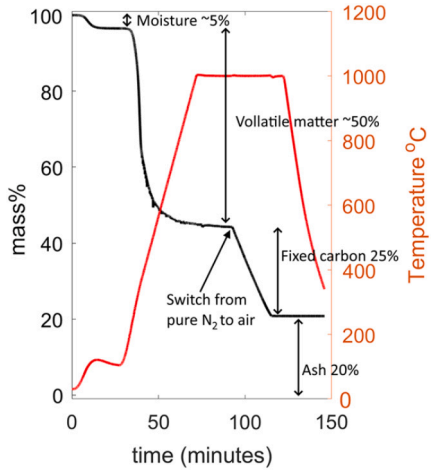

Fig. 1. Thermogravimetric analysis of lignin produced from Miscanthus Giganteus.

representation is given in the supplementary information) are shown in Table 2.

An overview of the adsorption effectiveness of these samples for 4 different PFAS is shown in the supplementary information, Tables S3 to S6. Unlike the result of Wang et al. (2023) (Wang et al., 2023), we found no enhancement of sorption effectiveness by short air treatment. On the contrary, the sorption of short chain PFAS (PFBA and PFBS) was greatly reduced by the treatment in air. It could be that our treatment was not 'short' enough, since there can be large variations between different ovens (The results of Wang's (2023) oxidation were obtained with a muffle furnace). We presume the introduction of new oxygen-containing surface groups caused this decrease in adsorption efficacy, due to increased electrostatic repulsion between the adsorbent surface and the PFAS compounds (Newcombe and Drikas, 1997). The negative influence of oxygen containing groups was also observed by Saeidi et al. (2021) (Saeidi et al., 2021). Complete treatment in air (4 hrs at 600 °C in air) created a material that did not adsorb any PFAS anymore. Coating the particles with a positively charged polyelectrolyte restored the adsorption capabilities to be similar to the nitrogen treated samples, more details on these samples are in the supplementary information.

3.2. Batch adsorption experiments

In order to assess the time needed for the batch adsorption experiments, a short kinetics test was performed. Samples with the same initial concentration of PFAS and same mass of adsorbent were shaken for different periods of time. The specific results from this can be found in the SI. For the bare lignin approximately 90 hours was needed to reach a stable equilibrium, but for all other tested materials no substantial change was observed after 24 hours. Therefore, stirring the vessels for at least 100 hours was assumed to be sufficient time to reach equilibrium for all PFAS concentrations and adsorbent types. Furthermore, experiments where the final concentrations were too low were excluded, since a small PFAS concentration (close to or below the limit of quantitation) can lead to large errors in estimating adsorption capacity.

The adsorption of the 4 different PFAS compounds onto miscanthus lignin and its carbonized version are shown in Figs. 2 and 3. All 4 PFAS compounds were added in a mix simultaneously. The range of initial concentrations was chosen to reflect a wide range of possible PFAS concentrations in water resources (Pistocchi and Loos, 2009; Boone et al., 2019). Although maximum adsorption capacity of the adsorbent can not be reliably estimated by this approach, the maximum adsorption capacity is of little interest if the concentration of contaminants for which it is estimated is almost never reached in practice. For none of the 4 compounds, at these low concentrations no indication of reaching the maximum adsorption capacity could be found. The distribution coefficients determined from linear isotherm fits are provided in Table 3.

When comparing the isotherms for PFOA adsorption in Figs. 2 and 3, an increase in sorption capacity of 2 orders of magnitude between lignin and carbonized lignin can be seen. This increase in sorption capacity can largely be attributed to the increase of the specific surface area of the material from 5.1 m^2/g to 140 m^2/g after carbonization. The rest of the adsorption capacity gain could be due surface alterations due to the carbonization process (e.g. due to decreased O/C ratio). As stated before, oxygen containing groups inhibit the adsorption of anionic PFAS onto carbonaceous adsorbents (Saeidi et al., 2021).

From Table 3 it can be seen that, as is expected, the distribution coefficient of shorter chain PFAS (PFBS and PFBA) was lower than that of PFOA and the distribution coefficient of PFOS was higher than that of PFOA. The reason for this is the difference in CF_2 chain length between the compounds (Fabregat-Palau et al., 2022). The CF_2 chain of PFOS is 1 segment longer than the CF_2 chain of PFOA and the CF_2 chain lengths of both PFBA and PFBS are shorter.

Comparing our K_D values with aggregate data on PFAS adsorption gathered recently by Navid Saeidi et al. shows that our values for activated carbon and carbonized lignin (biochar) are very comparable to the available FAIR data on PFAS adsorption (Saeidi et al., 2024). Navid Saeidi et al. report single point K_D values in the range of $10^{-}1$ to 10^4 L/g for PFAS compounds of varying length (Saeidi et al., 2024).

3.2.1. Ionic strength

One of the factors often found influencing PFAS adsorption is the ionic strength of the matrix (Stebel et al., 2019; Xiao et al., 2011). Higher ionic strength screens the electrostatic repulsion between the negative headgroup of the PFAS compound and the often negatively charged surface of the adsorbent material (e.g. in the case of many carbonaceous adsorbents) (Newcombe and Drikas, 1997). This effect should be larger for short-chain PFAS compared to long-chain PFAS, since the relative influence of the polar headgroup is larger (Aumeier et al., 2023). To assess the effect of the ionic strength on the PFAS sorption on carbonized lignin, isotherms were created at both low ionic strength (deionized water) and high ionic strength (100 mM KCl), see Figs. 4 and 5 (isotherms for PFBS and PFOS are available in the supplementary information). For the long-chain compounds (PFOA and PFOS) we observe partial saturation of the adsorbent at higher concentrations, therefore these data were fitted using a Langmuir isotherm. The carbonized lignin used for these experiments turned out to have a lower specific surface area (10.7 m^2/g), likely also contributing to the partial saturation of the adsorbent in this experiment. The fitting parameters can be found in Table 4. We

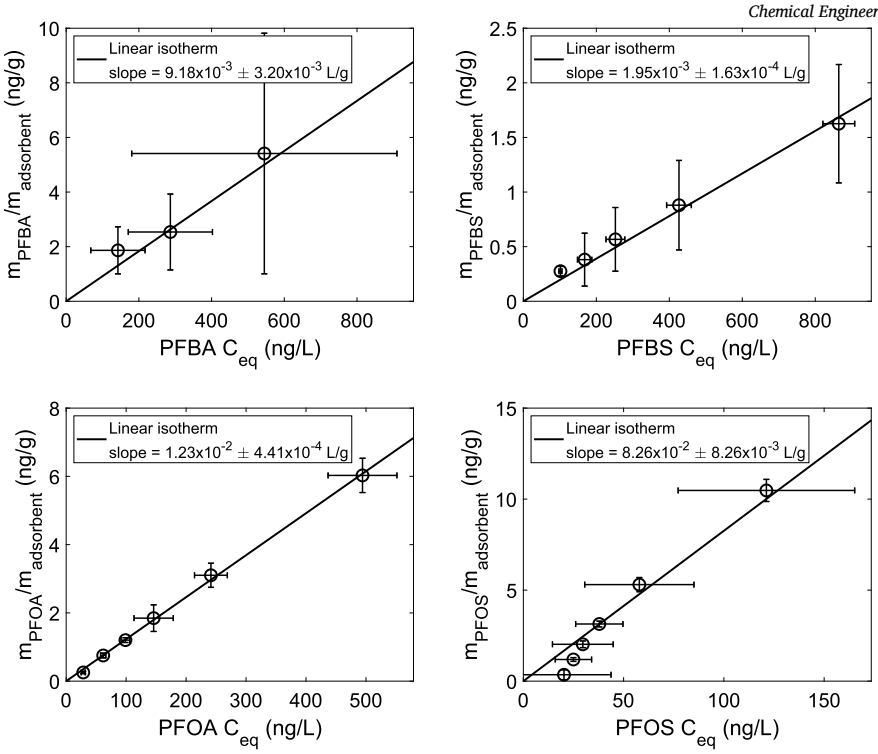

Fig. 2. Adsorption isotherms for PFBA, PFBS, PFOA and PFOS adsorption onto miscanthus lignin. Error bars are 95% confidence intervals based on 3 repeat samples. The fit parameter errors are 95% confidence intervals. The initial concentrations of the solutions were: 50, 125, 200, 300, 500 and 1000 ng/L (in a mix of 4 PFAS, all at the same concentration). Mean mass of adsorbent used was 1.26 ± 0.01 g (error based on difference in mass used from sample to sample) and the solution contained 100 mM KCl.

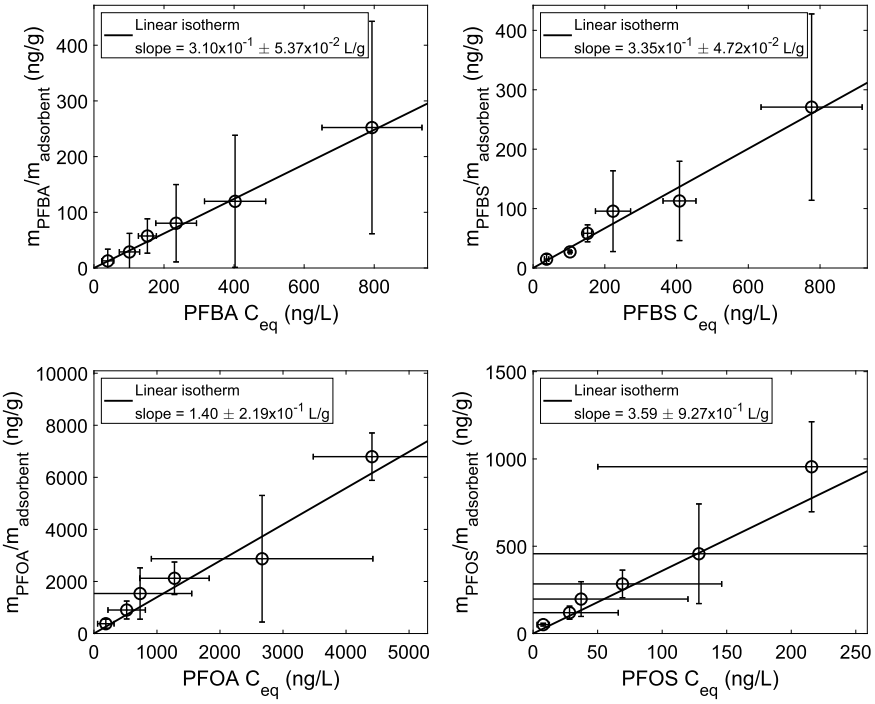

Fig. 3. Adsorption isotherms for PFBA, PFBS, PFOA and PFOS adsorption onto carbonized miscanthus lignin (specific surface area of 140 m^2/g). Error bars are 95% confidence intervals based on 3 repeat samples and fit parameter errors are 95% confidence intervals. The initial concentrations of the solutions were: 50, 125, 200, 300, 500 and 1000 ng/L (in a mixture of 4 PFAS and the initial concentration of PFOA was 10 times higher). Mean mass of adsorbent was $12.3x10^{-3}\pm 0.2x10^{-3}$ g (error based on difference in mass used from sample to sample) and the solutions contained 100 mM KCl.

only observe a significant increase in adsorption capacity due to high ionic strength for PFBA, and no significant effect for any of the other compounds. This coincides with the fact that for smaller PFAS the contribution of the polar headgroup is the largest and for longer chain PFAS the influence of the tail dominates (Aumeier et al., 2023). Therefore we did not find that ionic strength was a major factor influencing PFAS adsorption in general on carbonized lignin. From this we can conclude that the adsorption on carbonized lignin is mostly driven by hydrophobic in-

Table 3
Distribution coefficients of PFAS on lignin, carbonized lignin and activated carbon as determined from linear isotherm fits. Initial PFAS concentrations for these isotherm studies were 50, 125, 200, 300, 500 and 1000 ng/L.

Compound	K_D lignin (L/g)	K_D carbonized lignin (L/g)	K_D activated carbon (L/g)
PFBA	$9.18x10^{-3} \pm 3.20x10^{-3}$	$3.10x10^{-1} \pm 0.54x10^{-1}$	8.4 ± 6.4
PFBS	$1.95x10^{-3} \pm 0.16x10^{-3}$	$3.35x10^{-1} \pm 0.47x10^{-1}$	11.2 ± 4.3
PFOA	$1.23x10^{-2} \pm 4.41x10^{-4}$	1.40 ± 0.22	75.1 ± 47.2
PFOS	$8.26x10^{-2} \pm 0.83x10^{-2}$	3.59 ± 0.93	160.6 ± 59.8

Table 4
Fitting parameters of isotherms for PFAS sorption on carbonized lignin at varying ionic strengths. Parameter errors given are 95% confidence intervals.

Linear isotherm			
Compound	Ionic Strength (mM)	K_D (L/g)	
PFBA	0	0.18 ± 0.05	
PFBA	100	0.40 ± 0.03	
PFBS	0	0.29 ± 0.06	
PFBS	100	0.29 ± 0.04	
Langmuir isotherm			
Compound	Ionic Strength (mM)	K_D (L/g)	Nmax (ng/g)
PFOA	0	4.3 ± 2.2	8118 ± 2569
PFOA	100	4.3 ± 1.1	13611 ± 6800
PFOS	0	72 ± 22	2509 ± 459
PFOS	100	139 ± 73	2222 ± 355

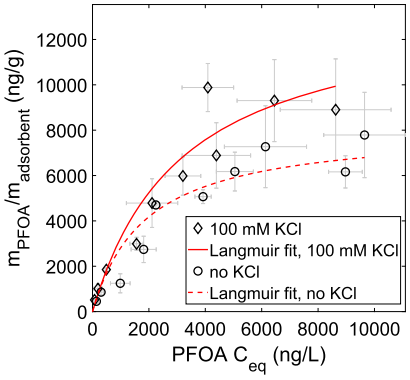

Fig. 4. Effect of ionic strength on PFOA adsorption on carbonized lignin particles (specific surface area of 10.7 m^2/g). Error bars show the standard deviation of 3 repeat samples for each initial PFAS concentration. Experimental details: $12.3x10^{-3} \pm 0.2x10^{-3}$ g of carbonized lignin as adsorbent, the initial PFAS concentrations of each individual compound were 500, 1000, 2000, 4000, 6000, 8000, 10000, 12000, 14000 and 16000 ng/L and the volume of the PFAS solution was 15 mL.

teractions and electrostatic interactions play a minor role. However, as there is a significant effect for PFBA, the relevance of electrostatic interactions could be even more pronounced for even smaller PFAS (Aumeier et al., 2023).

Olhansky et al. see a decrease in adsorption capacity with increasing ionic strength, and concurrent with our results this effect is most precedented <100 mM ionic strength (Olshansky et al., 2022). This behavior is expected for their cationically charged adsorbents, since the larger amount of ions will screen the surface charges and therefore weaken electrostatic interactions between the adsorbent and PFAS.

3.3. Rapid small scale column tests

Rapid small scale column tests (RSSCT) were performed to determine the dynamic capacity of the carbonized lignin, in order to compare it to a commercial activated carbon material. By doing dynamic experiments

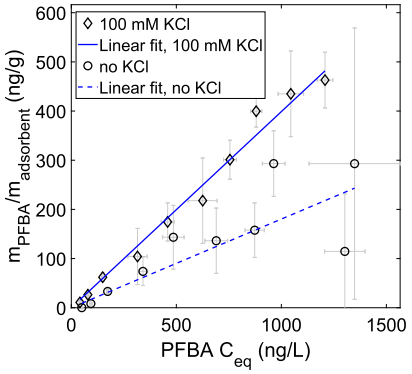

Fig. 5. Effect of ionic strength on PFBA adsorption on carbonized lignin particles (specific surface area of 10.7 m^2/g). Error bars show the standard deviation of 3 repeat samples for each initial PFAS concentration. Experimental details: $12.3x10^{-3} \pm 0.2x10^{-3}$ g of carbonized lignin as adsorbent, the initial PFAS concentrations of each individual compound were 50, 100, 200, 400, 600, 800, 1000, 1200, 1400 and 1600 ng/L and the volume of the PFAS solution was 15 mL.

instead of static batch experiments it is possible to more closely mimic larger scale application of adsorption processes and provide information of the kinetics of adsorption on the material, although there can be substantial differences between columns of varying sizes (Juela et al., 2022). Results of our rapid small scale column experiments are shown in Fig. 6 and 7 for PFOA, for both carbonized lignin and activated carbon respectively (experimental conditions can be found in Table 5). The breakthrough curves for the other compounds are shown in the supplementary information.

Although the curves are not perfectly symmetrical breakthrough curves (this is common in small column experiments), using the Thomas model (Chu, 2010) with assuming a linear isotherm (equation (4)), we were able to describe our results when using carbonized lignin. Using the distribution coefficient found in the batch experiments (for PFOA 1.4 L/g) and fitting $\kappa\epsilon$ (if ϵ could be determined separately, the rate constant κ can be estimated). For PFOS on carbonized lignin (shown in the supplementary information) we could not adequately describe our data using the linear Thomas model, so we instead opted to use equation (9). Fixing the distribution coefficient to the value obtained from the batch experiments (although this was obtained from a linear isotherm), giving us a value of $\kappa\epsilon$ very close to the ones for the other compounds, see Table 6. The large variations in specific surface area of the carbonized lignin material (see the supplementary information) could be the cause for not getting linear isotherm behavior in this case for PFOS.

The same experiment using the same amount of mass of commercial activated carbon resulted in Fig. 7. Even though the experiment was performed for much longer (also considering the bed volume is more than twice as large), the inlet concentration ($C/C_0 = 1$) is never attained for PFOA. In order to achieve these large volumes, long times (several days) were required and the flowrate had to be lowered (to 0.03 mL/min, 10 times lower) overnight due to limitations of the setup. We can see a breakthrough of PFOA after approximately 500 bed volumes however, where for the carbonized lignin there was instantaneous breakthrough.

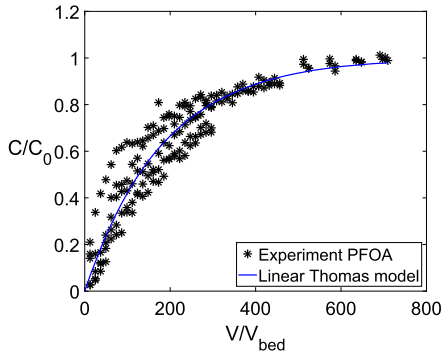

Fig. 6. Results of rapid small scale column test using 70 mg of carbonized lignin (specific surface area is 140 m^2/g). Experimental conditions can be found in Table 5.

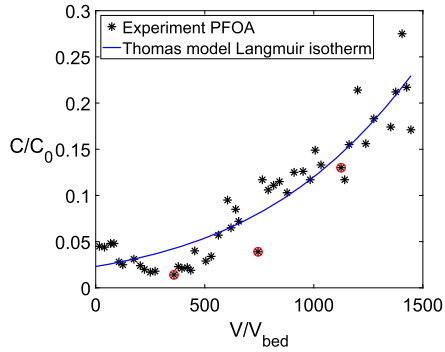

Fig. 7. Results of rapid small scale column test using 70 mg of activated carbon. Colored circles indicate samples that were taken after running the column over night at 1/10th of the flowrate. Experimental conditions can be found in Table 5.

Table 5
Experimental conditions for rapid small scale column tests. [a] a diffusion coefficient of $5x10^{-10}$ m^2/s was assumed for all compounds (Pereira et al., 2014; Damião et al., 2023). [b] empty bed contact time.

Property	Carbonized lignin columns	Activated carbon columns
Diameter (cm)	1.26	1.26
Length (cm)	0.13	0.3
Flow rate (mL/min)	0.3	0.3
Superficial velocity (m/s)	$4.2x10^{-5}$	$4.2x10^{-5}$
Peclet number[a]	109	251
EBCT[b] (s)	32.4	71.4
ρ_s (g/L)	$1.94x10^3$	$1.99x10^3$

From these experiments it seems the findings for our values of the distribution coefficient seem to also hold in a column adsorption setting. There is no indication that either of the adsorbents behaves very differently, as the $\kappa\epsilon$ values are very similar for both particles. From this we conclude that our values of the distribution coefficients are a good indicator of the capability of the adsorbent material to remove PFAS at low concentrations. From the breakthrough curves for both materials tested at similar conditions, it seems that there is substantial breakthrough (C/C0 = 0.2 is chosen here as comparison point) of PFOA through carbonized lignin after already 50 bed volumes, while for activated carbon (Norit) this is after 1400 bed volumes. This indicates that the activated carbon here functions about 30 times better than the carbonized lignin particles in a similar setting, which is comparable to their difference in surface area.

3.4. Applicability of bio-sorbents for PFAS remediation

Although the tested bio-sorbents have substantially lower surface areas compared to commercial activated carbons (see Table 1), their benefits from both a environmental and cost standpoint can outweigh this. Doing an extensive life cycle assessment study of all the processes which produce the bio-sorbents is outside of the scope of this study, but still initial estimations can be performed.

Table 6
Fitting parameters from Thomas model, either based on a linear isotherm or Langmuir isotherm. Values of K_D were used from the batch experiments.

Compound	$\kappa\epsilon$ (1/s)	N_{max} (ng/g)	Isotherm
Carbonized Lignin (n = 5)			
PFBA	0.71 ± 0.12	-	Linear isotherm
PFBS	0.22 ± 0.02	-	Linear isotherm
PFOA	0.23 ± 0.01	-	Linear isotherm
PFOS	0.10 ± 0.01	181 ± 6	Langmuir isotherm
Activated Carbon (n = 1)			
PFBA	0.27 ± 0.03	-	Linear isotherm
PFBS	0.08 ± 0.01	584 ± 34	Langmuir isotherm
PFOA	0.12 ± 0.01	864 ± 60	Langmuir isotherm
PFOS	0.13 ± 0.02	1053 ± 197	Langmuir isotherm

Activated carbon production is an energy intensive process that consumes a large quantity of fossil fuels, leading to an estimated global warming potential (GWP) of approximately 10-20 kg CO_2-eq per kg of activated carbon produced (Kim et al., 2019; EU consortium PortableCrac, 2018). In this case we will use a value of 13.16 kg CO_2-eq per kg of activated carbon produced as determined in the European Portablecrac project (EU consortium PortableCrac, 2018). Additionally we add 2.6 kg CO_2-eq per kg of activated carbon as a GWP cost for discarding the material, which was the determined value for thermal reactivation from the same project (although we do not consider adsorbent regeneration) (EU consortium PortableCrac, 2018). Adding these values gives us an estimated GWP of 15.8 kg CO_2-eq per kg of activated carbon.

Life cycle assessments for the production of bio-based adsorbents are less common and show great variations in results (Moretti et al., 2021). For both lignin (Moretti et al., 2021) and cellulosic fibres (Shen et al., 2010) the values range from 0.5-5 kg CO_2-eq per kg of material. However, a very common range is approximately 2 kg CO_2-eq per kg of material, generally given as cradle-to-gate values (start of lifecycle to finished product, disregarding use and end of lifecycle) (Moretti et al., 2021). Assuming that it is likely that these adsorbents will be burned after use an additional end of life factor is incorporated:

$$\text{GWP bio-sorbent} = 2 + \frac{m_{CO_2}}{m_C}\frac{\text{wt\%}C_{sorbent}}{100\%} = 2 + \frac{44}{12}\frac{70\%}{100\%} = 4.6 \qquad (13)$$

The carbon content of 70% for the bio-based adsorbent is based on aggregated data collected by Thauront et al. (Thauront et al., 2024). This results in 4.6 kg CO_2-eq per kg of bio-based adsorbent. Therefore, in order to break even based on global warming potential the adsorption capacity of the bio-based adsorbents would have to be about $\frac{4.6}{15.8}$ = 30% of that of activated carbons. For the adsorbents we have investigated this was not the case, as the carbonized lignin performed 30 times worse than the activated carbon in the column tests. The capacity of the biobased adsorbent in this case is therefore only 3% of the activated carbon, meaning there is a factor 10 improvement needed to be on par with activated carbons, which is in line with the about factor 10 difference in specific surface areas of the materials.

Additionally in terms of costs, the production of activated carbons is estimated to cost around €2 per kg (Viegas et al., 2019; León et al., 2020). In contrast, the costs of production of bio-based adsorbents are more difficult to define. As an example, the wide range of lignin qualities leads to a price range from €0.05 to €0.75 per kg, although the highest cost lignin is produced only in small volume and therefore not likely to be suitable sources of bio-sorbent (Gosselink, 2011). Since these estimations might be outdated, we opt for a more conservative estimation of €0.40 per kg for lignin to be used as an adsorbent, based on price ranges for sulfonated lignin, kraft lignin and soda lignin (Gosselink, 2011). This

Table 7
Numbers used for calculations shown in Fig. 8. The indicated colors refer to colors used in Fig. 8. SSA: specific surface area. GWP: global warming potential in CO_2 equivalents.

Material	SSA (m^2/g)	GWP (kg_{CO_2}/kg)
Lignin base	5.1	4.6
Carbonized lignin	variable	4.6 (black) / 7.6 (red)
Activated carbon	1592	15.8

does not consider the costs of carbonization/activation to increase the adsorbents capacity. Again here there is only a factor 5 benefit of using lignin over activated carbon in terms of cost, which is considerably smaller than the factor 30 worse performance we observed in our rapid small scale column testing.

Therefore from both a global warming potential and cost comparison, it seems that in order for these materials to be on par with conventional activated carbons the adsorption capacity should be at least one third of that of conventional activated carbon based on our GWP estimations and one fifth based on our cost estimations. Since the adsorption capacity of PFAS compounds for carbonaceous adsorbents seems to be mostly related to the specific surface area of the material, we compared the specific surface area divided by the GWP of a material to get an idea of the applicability of lignin/cellulose bio-materials as adsorbent materials, see Fig. 8 (Saeidi et al., 2024). Numbers used for these calculations can be found in Table 7. From this figure we can see that in order to be on par with conventional activated carbon materials (solid black line), bio-based adsorbents need to also be produced with high surface areas (>1000 m^2/g), while retaining >50% of their original mass. As can be seen from Tables 1 and 2, our carbonized lignin is far away from this threshold. Since our material consists of 50% vollatile matter (see Fig. 1), it is unlikely that retaining more than 50% of the original mass is feasible at all using this lignin product. From the TGA results in Fig. 1 we can however conclude that thermal regeneration of the carbonized lignin is possible, as the mass loss at high temperature (1000 °C) is not substantial. The dashed lines in Fig. 8 show the effectiveness of carbonization vs using the base material, indicating that even when the final surface area is not in the range of 1000 m^2/g, carbonization is still preferable over using the base material as an adsorbent.

Many methods exist to create porous carbons with large surface areas from carbon materials (Gayathiri et al., 2022). Common methods to increase the specific surface area and pore volume include physical activation (e.g. with steam or CO_2) or chemical activation (e.g. with $ZnCl_2$, KOH or H_3PO_4) (Gayathiri et al., 2022). Even though these methods increase the adsorption capacity and kinetics of the final product, the yield is generally decreased (Bergna et al., 2022). Bergna et al. (2022) have shown that producing bio-based carbonaceous materials with a high surface area (1000 - 2000 m^2/g) is possible from lignin, showing the trade-off between specific surface area and final adsorbent yield (Bergna et al., 2022).

4. Conclusion

Replacing conventional (fossil based) activated carbon materials by bio-based adsorbents for PFAS adsorption requires thorough investigation of the adsorption capacity of these adsorbents. From our selection of bio-based materials tested for PFAS adsorption, lignin was the best performing material. Adsorption was mostly driven by hydrophobic interactions, as indicated by the major effect of the specific surface area and the minor effect of the ionic strength on the adsorption capacity. However due to the low specific surface area of these unmodified materials, the adsorption capacity is not sufficient to be on par with conventional activated carbon, even though the materials are more sustainably produced. By carbonizing the lignin we were able to increase the adsorption capacity by 1 to 2 orders of magnitude (depending on the PFAS compound), however this was still not enough to compete with activated carbon. We estimated that in order to create an adsorbent based on lignin that is on par with activated carbon on from a global warming point of view, an adsorbent with a specific surface area of at least 1000 m^2/g would be needed, while retaining at least 50% of the initial mass.

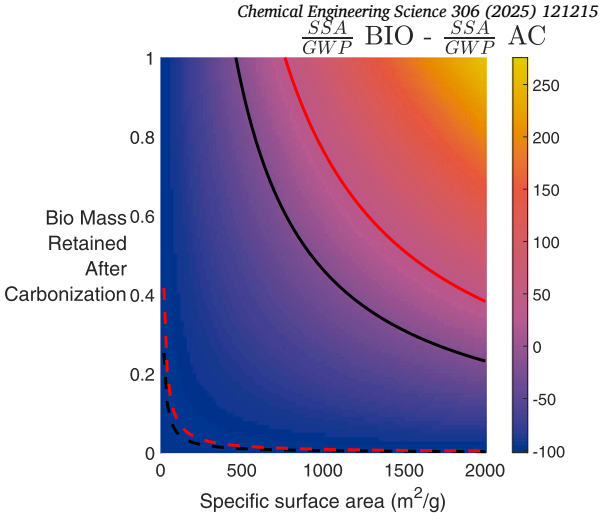

Fig. 8. Viability of bio-based adsorbents compared to conventional activated carbon as adsorbent material. A positive number indicates the bio-based adsorbent has a likely lower GWP than using a conventional activated carbon. The solid line is the border of AC-preferred to bio-based prefered and the dashed line indicates where carbonization of the bio-based material starts to improve it's SSA/GWP compared to the base material. The red lines are a scenario where 3 kg_{CO_2}/kg GWP was added for carbonizing lignin.

CRediT authorship contribution statement

J.B. Roman: Writing – original draft, Visualization, Validation, Methodology, Investigation, Formal analysis, Conceptualization. **A.J.B. Kemperman:** Writing – review & editing, Writing – original draft, Supervision, Conceptualization. **W.G.J. van der Meer:** Writing – review & editing, Supervision, Funding acquisition, Conceptualization. **J.A. Wood:** Writing – review & editing, Supervision, Funding acquisition, Conceptualization.

Funding sources

The authors thank Oasen N.V., a Dutch drinking water company, for funding this work.

Declaration of competing interest

The authors declare the following financial interests/personal relationships which may be considered as potential competing interests: Walter G.J. van der Meer was CEO until Feb. 1st, 2024 of Oasen N.V., who funded this work. The other authors declare that they have no known competing financial interests or personal relationships that could have appeared to influence the work reported in this paper.

Acknowledgements

The authors gratefully acknowledge funding of this work by Oasen N.V. (the Netherlands). We thank the JRS group for providing us samples of cellulose fibres for usage in the project. The authors thank dr. Esra te Brinke for her help in using the HPLC-MS system and ir. Mike Essink and Koen Putman for their contributions to the experimental work.

Appendix A. Supplementary material

Supplementary material related to this article can be found online at https://doi.org/10.1016/j.ces.2025.121215.

Data availability

Data will be made available on request.

References

Agency for Toxic Substances and Disease Registry (ATSDR), 2021. Toxicological profile for perfluoroalkyls. U.S. Department of Health and Human Services, Public Health Service, Atlanta, GA. https://doi.org/10.15620/cdc:59198.

EU consortium PortableCrac, 2018. Lca & lcca of acquiring virgin ac and of thermal regeneration. https://doi.org/10.3030/768905.

Appleman, T.D., Higgins, C.P., Quiñones, O., Vanderford, B.J., Kolstad, C., Zeigler-Holady, J.C., Dickenson, E.R., 2014. Treatment of poly- and perfluoroalkyl substances in U.S. full-scale water treatment systems. Water Res. 51, 246–255.

Aumeier, B.M., Georgi, A., Saeidi, N., Sigmund, G., 2023. Is sorption technology fit for the removal of persistent and mobile organic contaminants from water? Sci. Total Environ. 880, 163343.

Benstoem, F., Nahrstedt, A., Boehler, M., Knopp, G., Montag, D., Siegrist, H., Pinnekamp, J., 2017. Performance of granular activated carbon to remove micropollutants from municipal wastewater—a meta-analysis of pilot- and large-scale studies. Chemosphere 185, 105–118.

Bergna, D., Varila, T., Romar, H., Lassi, U., 2022. Activated carbon from hydrolysis lignin: effect of activation method on carbon properties. Biomass Bioenergy 159, 106387.

Bolster, C.H., 2008. Revisiting a statistical shortcoming when fitting the Langmuir model to sorption data. J. Environ. Qual. 37, 1986–1992.

Boone, J.S., Vigo, C., Boone, T., Byrne, C., Ferrario, J., Benson, R., Donohue, J., Simmons, J.E., Kolpin, D.W., Furlong, E.T., Glassmeyer, S.T., 2019. Per- and polyfluoroalkyl substances in source and treated drinking waters of the United States. Sci. Total Environ. 653, 359–369.

Buckley, T., Karanam, K., Han, H., Vo, H.N.P., Shukla, P., Firouzi, M., Rudolph, V., 2023. Effect of different co-foaming agents on pfas removal from the environment by foam fractionation. Water Res. 230, 119532.

Calafat, A.M., Wong, L.Y., Kuklenyik, Z., Reidy, J.A., Needham, L.L., 2007. Polyfluoroalkyl chemicals in the U.S. population: data from the national health and nutrition examination survey (nhanes) 2003–2004 and comparisons with nhanes 1999–2000. Environ. Health Perspect. 115, 1596.

Chen, Y., Zhang, H., Liu, Y., Bowden, J.A., Tolaymat, T.M., Townsend, T.G., Solo-Gabriele, H.M., 2022. Concentrations of perfluoroalkyl and polyfluoroalkyl substances before and after full-scale landfill leachate treatment. Waste Manag. 153, 110–120.

Chu, K.H., 2010. Fixed bed sorption: setting the record straight on the Bohart–Adams and Thomas models. J. Hazard. Mater. 177, 1006–1012.

Damião, G., Morgado, P., Silva, P., Martins, L.F., McCabe, C., Filipe, E.J., 2023. Perfluorinated pollutants in water: diffusion coefficient of perfluorosulfonic acids by molecular dynamics simulations. Fluid Phase Equilib. 575, 113928.

Fabregat-Palau, J., Vidal, M., Rigol, A., 2022. Examining sorption of perfluoroalkyl substances (pfas) in biochars and other carbon-rich materials. Chemosphere 302, 134733.

Felizeter, S., McLachlan, M.S., de Voogt, P., 2012. Uptake of perfluorinated alkyl acids by hydroponically grown lettuce (lactuca sativa). Environ. Sci. Technol. 46, 11735–11743.

Franke, V., Ullberg, M., McCleaf, P., Wålinder, M., Köhler, S.J., Ahrens, L., 2021. The price of really clean water: combining nanofiltration with granular activated carbon and anion exchange resins for the removal of per- and polyfluoralkyl substances (pfass) in drinking water production. ACS ES&T Water 1, 782–795.

Gagliano, E., Sgroi, M., Falciglia, P.P., Vagliasindi, F.G., Roccaro, P., 2020. Removal of poly- and perfluoroalkyl substances (pfas) from water by adsorption: role of pfas chain length, effect of organic matter and challenges in adsorbent regeneration. Water Res. 171, 115381.

Gayathiri, M., Pulingam, T., Lee, K., Sudesh, K., 2022. Activated carbon from biomass waste precursors: factors affecting production and adsorption mechanism. Chemosphere 294, 133764.

Gosselink, R.J.A., 2011. Lignin as a renewable aromatic resource for the chemical industry. Ph.D. thesis. Wageningen University & Research. https://edepot.wur.nl/186285.

Hiester, N.K., Vermeulen, T., 1952. Saturation performance of ion-exchange and adsorption columns. Chem. Eng. Prog. 48, 505–516.

Hubbe, M.A., 2021. Insisting upon meaningful results from adsorption experiments. Sep. Purif. Rev. https://doi.org/10.1080/15422119.2021.1888299.

Juela, D., Vera, M., Cruzat, C., Astudillo, A., Vanegas, E., 2022. A new approach for scaling up fixed-bed adsorption columns for aqueous systems: a case of antibiotic removal on natural adsorbent. Process Saf. Environ. Prot. 159, 953–963.

Kaiser, A.M., Aro, R., Kärrman, A., Weiss, S., Hartmann, C., Uhl, M., Forsthuber, M., Gundacker, C., Yeung, L.W., 2020. Comparison of extraction methods for per- and polyfluoroalkyl substances (pfas) in human serum and placenta samples—insights into extractable organic fluorine (eof). Anal. Bioanal. Chem. 413, 865–876.

Kim, M.H., Jeong, I.T., Park, S.B., Kim, J.W., 2019. Analysis of environmental impact of activated carbon production from wood waste. Environ. Eng. Res. 24, 117–126.

Kotthoff, M., Müller, J., Jürling, H., Schlummer, M., Fiedler, D., 2015. Perfluoroalkyl and polyfluoroalkyl substances in consumer products. Environ. Sci. Pollut. Res. 22, 14546–14559.

Kumarasamy, E., Manning, I.M., Collins, L.B., Coronell, O., Leibfarth, F.A., 2020. Ionic fluorogels for remediation of per- and polyfluorinated alkyl substances from water. ACS Cent. Sci. 6, 487–492.

Langmuir, I., 1918. The adsorption of gases on plane surfaces of glass, mica and platinum. J. Am. Chem. Soc. 40, 1361–1403.

León, M., Silva, J., Carrasco, S., Barrientos, N., 2020. Design, cost estimation and sensitivity analysis for a production process of activated carbon from waste nutshells by physical activation. Processes 2020 (8), 945.

Li, D., Londhe, K., Chi, K., Lee, C.-S., Venkatesan, A.K., Hsiao, B.S., Venkatesan, C.K.A., 2021. Functionalized bio-adsorbents for removal of perfluoroalkyl substances: a perspective. AWWA Water Sci. 3, e1258.

Li, J., Sun, J., Li, P., 2022. Exposure routes, bioaccumulation and toxic effects of per- and polyfluoroalkyl substances (pfass) on plants: a critical review. Environ. Int. 158, 106891.

Mantripragada, S., Obare, S.O., Zhang, L., 2022. Addressing short-chain pfas contamination in water with nanofibrous adsorbent/filter material from electrospinning. Acc. Chem. Res. 08, 47.

McCleaf, P., Englund, S., Östlund, A., Lindegren, K., Wiberg, K., Ahrens, L., 2017. Removal efficiency of multiple poly- and perfluoroalkyl substances (pfass) in drinking water using granular activated carbon (gac) and anion exchange (ae) column tests. Water Res. 120, 77–87.

McCleaf, P., Stefansson, W., Ahrens, L., 2023. Drinking water nanofiltration with concentrate foam fractionation—a novel approach for removal of per- and polyfluoroalkyl substances (pfas). Water Res. 232, 119688.

Moretti, C., Corona, B., Hoefnagels, R., Vural-Gürsel, I., Gosselink, R., Junginger, M., 2021. Review of life cycle assessments of lignin and derived products: lessons learned. Sci. Total Environ. 770, 144656.

Nakayama, S.F., Hasegawa, T., 2023. Pfas science and regulation should be reconsidered using fluorine-specific physical chemistry.

Newcombe, G., Drikas, M., 1997. Adsorption of nom onto activated carbon: electrostatic and non-electrostatic effects. Carbon 35, 1239–1250.

Olshansky, Y., Gomeniuc, A., Chorover, J., Abrell, L., Field, J.A., Hatton, J., He, J., Sierra-Alvarez, R., 2022. Tailored polyanilines are high-affinity adsorbents for per- and polyfluoroalkyl substances. ACS ES&T Water 2, 1402–1410.

Pereira, L.A.M., Martins, L.F.G., Ascenso, J.R., Morgado, P., Ramalho, J.P.P., Filipe, E.J.M., 2014. Diffusion coefficients of fluorinated surfactants in water: experimental results and prediction by computer simulation. J. Chem. Eng. Data 59, 3151–3159.

Pistocchi, A., Loos, R., 2009. A map of European emissions and concentrations of pfos and pfoa. Environ. Sci. Technol. 43, 9237–9244.

Saeidi, N., Kopinke, F.-D., Georgi, A., 2021. What is specific in adsorption of perfluoroalkyl acids on carbon materials? Chemosphere 273, 128520.

Saeidi, N., Lai, A., Harnisch, F., Sigmund, G., 2024. A fair comparison of activated carbon, biochar, cyclodextrins, polymers, resins, and metal organic frameworks for the adsorption of per- and polyfluorinated substances. Chem. Eng. J. 498, 155456.

Schrenk, D., Bignami, M., Bodin, L., Chipman, J.K., del Mazo, J., Grasl-Kraupp, B., Hogstrand, C., Hoogenboom, L.R., Leblanc, J., Nebbia, C.S., Nielsen, E., Ntzani, E., Petersen, A., Sand, S., Vleminckx, C., Wallace, H., Barregård, L., Ceccatelli, S., Cravedi, J., Halldorsson, T.I., Haug, L.S., Johansson, N., Knutsen, H.K., Rose, M., Roudot, A., Loveren, H.V., Vollmer, G., Mackay, K., Riolo, F., Schwerdtle, T., 2020. Risk to human health related to the presence of perfluoroalkyl substances in food. EFSA J. 18.

Schulz, K., Silva, M.R., Klaper, R., 2020. Distribution and effects of branched versus linear isomers of pfoa, pfos, and pfhxs: a review of recent literature. Sci. Total Environ. 733, 139186.

Shahrokhi, R., Park, J., 2024. Enhanced removal of short- and long-chain per- and polyfluoroalkyl substances from aqueous phase using crushed grafted chitosan beads: performance and mechanisms. Environ. Pollut. 340, 122836.

Shen, L., Worrell, E., Patel, M.K., 2010. Environmental impact assessment of man-made cellulose fibres. Resour. Conserv. Recycl. 55, 260–274.

Stebel, E.K., Pike, K.A., Nguyen, H., Hartmann, H.A., Klonowski, M.J., Lawrence, M.G., Collins, R.M., Hefner, C.E., Edmiston, P.L., 2019. Absorption of short-chain to long-chain perfluoroalkyl substances using swellable organically modified silica. Environ. Sci. Water Res. Technol. 5, 1854–1866.

Thauront, J.L., Soja, G., Schmidt, H., Abiven, S., 2024. A critical re-analysis of biochar properties prediction from production parameters and elemental analysis. GCB Bioenergy 16.

Thomas, H.C., 1948. Chromatography: a problem in kinetics. Ann. N.Y. Acad. Sci. 49, 161–182.

Vakili, M., Bao, Y., Gholami, F., Gholami, Z., Deng, S., Wang, W., Awasthi, A.K., Rafatullah, M., Cagnetta, G., Yu, G., 2021. Removal of hfpo-da (genx) from aqueous solutions: a mini-review. Chem. Eng. J. 424, 130266.

Verduzco, R., Wong, M.S., 2020. Fighting pfas with pfas. ACS Cent. Sci. 6, 453–455.

Viegas, R.M., Mesquita, E., Campinas, M., Rosa, M.J., 2019. Pilot studies and cost analysis of hybrid powdered activated carbon/ceramic microfiltration for controlling pharmaceutical compounds and organic matter in water reclamation. Water 2020 (12), 33.

Wackett, L.P., 2021. Nothing lasts forever: understanding microbial biodegradation of polyfluorinated compounds and perfluorinated alkyl substances. Microb. Biotechnol. 15.

Wang, B., Sun, D., Yuan, T.Q., Song, G., Sun, R.C., 2021. Recent advances in lignin modification and its application in wastewater treatment. In: Lignin Utilization Strategies: From Processing to Applications. American Chemical Society, pp. 143–173.

Wang, W., Mi, X., Zhou, Z., Zhou, S., Li, C., Hu, X., Qi, D., Deng, S., 2019. Novel insights into the competitive adsorption behavior and mechanism of per- and polyfluoroalkyl substances on the anion-exchange resin. J. Colloid Interface Sci. 557, 655–663.

Wang, Z., Alinezhad, A., Sun, R., Xiao, F., Pignatello, J.J., 2023. Pre- and postapplication thermal treatment strategies for sorption enhancement and reactivation of biochars for removal of per- and polyfluoroalkyl substances from water. ACS ES&T Eng. 3, 193–200.

Whitehead, H.D., Venier, M., Wu, Y., Eastman, E., Urbanik, S., Diamond, M.L., Shalin, A., Schwartz-Narbonne, H., Bruton, T.A., Blum, A., Wang, Z., Green, M., Tighe, M., Wilkinson, J.T., McGuinness, S., Peaslee, G.F., 2021. Fluorinated compounds in North American cosmetics. Environ. Sci. Technol. Lett. 8, 538–544.

Xiao, F., Zhang, X., Penn, L., Gulliver, J.S., Simcik, M.F., 2011. Effects of monovalent cations on the competitive adsorption of perfluoroalkyl acids by kaolinite: experimental studies and modeling. Environ. Sci. Technol. 45, 10028–10035.

Yuan, J., Mortazavian, S., Passeport, E., Hofmann, R., 2022. Evaluating perfluorooctanoic acid (pfoa) and perfluorooctanesulfonic acid (pfos) removal across granular activated carbon (gac) filter-adsorbers in drinking water treatment plants. Sci. Total Environ. 838, 156406.

Zhang, Y., Tan, X., Lu, R., Tang, Y., Qie, H., Huang, Z., Zhao, J., Cui, J., Yang, W., Lin, A., 2022. Enhanced Removal of Polyfluoroalkyl Substances by Simple Modified Biochar: Adsorption Performance and Theoretical Calculation. ACS ES and T Water.